РАЗДЕЛ ТРЕТИЙ

МАТЕРИАЛЫ ПЕРСПЕКТИВНЫХ ЯДЕРНЫХ РЕАКТОРОВ

УДК 669.15-194

ODS STEEL AS STRUCTURAL MATERIAL FOR HIGH TEMPERATURE NUCLEAR REACTORS

M.A. Pouchon, M. Döbeli, R. Schelldorfer, J. Chen, W. Hoffelner, C. Degueldre
Paul Scherrer Institute, 5232 Villigen PSI, Switzerland

Oxide dispersed strengthened (ODS) ferritic-martensitic steels are investigated as possible structural material for the future generation of High Temperature Gas Cooled Nuclear Reactors. The Ni based austenitic ODS superalloys are not considered, because of the Ni presence, which is unfavorable under neutron irradiation. ODS-steels are considered to replace other high temperature materials for tubing or structural parts. Interestingly, ODS is also considered as material being used in future fusion applications. The oxide particles serve for interfacial pinning of moving dislocations. Therefore the creep resistance is improved. In case of the usage of these materials in reactor, the behavior under irradiation must be further clarified. In this paper the effects induced by He implantation are investigated. The induced swelling is measured and the mechanical behavior of the irradiated surface is investigated. These first tests are performed at room temperature, where a clear swelling and hardening could be observed.

1. INTRODUCTION

1.1. THE HIGH TEMPERATURE PROJECT

The temperature of current light water reactors (LWR) does not exceed 350 ºC. Energy conversion is done by steam generation and steam turbines. Materials for these applications exist. Research focuses mainly on safety and life assessment under fuel high burnup conditions and reactor ageing. In contrast to the LWRs, concepts for future (generation IV) nuclear fission plants focus on much higher temperatures necessary to increase the thermal cycle efficiency and to include process heat applications (e.g. hydrogen production). Fast neutron spectra are also considered. Concepts for nuclear plants are studied world wide within the framework of the Generation IV international forum (GIF), of which Switzerland is also full member.

1.2. PM2000 AS POTENTIAL MATERIAL

The role of ODS-materials for fusion applications was reviewed by Ukai and Fujiwara [2] and also by Hoelzer [3]. Both conclude that ODS materials are interesting for future nuclear applications. It is worth mentioning that ODS materials have not been considered for HTRs so far. They have, however, proven their capabilities with respect to high temperature gas cooled reactor applications in the meanwhile and they should be considered as serious candidates for future nuclear high temperature applications according to the opinion of the members of the GIF VHTR and GFR Steering Committees and researchers from FZ Jülich [4]and Petten [5].

PM2000 is an oxide dispersion strengthened (ODS) alloy of the composition 20 wt% Cr, 5.5 wt% Al, 0.5 wt% Ti, 0.5 wt% Y_2O_3, balance Fe, manufactured by mechanically alloying in a high energy mill to produce a solid solution which contains a uniform dispersion of yttria. The powder is consolidated using hot isostatic pressing followed by a hot and cold rolling procedure. Then a thermal treatment finalizes the production [6,7].The alloy is supplied by Plansee GmbH.

2. EXPERIMENTAL

2.1. SAMPLE PREPARATION

PM2000 ODS samples are cut and polished in the following way. Several samples of the dimension 6 x 6 x 1 mm are cut in a long transverse direction. One surface is then ground with SiC papers down to a P-Grading of 4000. A polishing with a 6 and 3 μm diamond suspension is performed, and the polishing is then finalized with OPS for 2'.

2.2. IRRADIATION

The samples described in Section 2.1. are irradiated with a $^4He^{++}$ beam at the Swiss Federal Institute of Technology in Zürich, using a Tandem Accelerator. The main difference from a thermal neutron irradiation is the high He to dpa ratio, however, for this preliminary study this fact was accepted and the data gained from this experiment also represents an extreme situation, which might be faced in a fast spectrum. For further information about the simulation of n irradiation by charged particles, see [7]. An even distribution is desirable; therefore the irradiation is performed under 4 different incident angles (ranging from 0° to 66°) and an energy of 1.5 MeV. The damage as a function of depth is then already quite even, being about 0.7 to 1.3 dpa from 1 to 2.5 μm. Figure 1,a) shows a TRIM simulation of the induced damage profile. TRIM tends to underestimate the width of the implantation-profile and the peaks appear sharper than in reality.

ВОПРОСЫ АТОМНОЙ НАУКИ И ТЕХНИКИ. 2005. № 3.
Серия: Физика радиационных повреждений и радиационное материаловедение (86), с. 122-127.

The irradiated fluences are $1.4 \cdot 10^{16}$, $2.8 \cdot 10^{16}$, $5.6 \cdot 10^{16}$ and $1.12 \cdot 10^{17}$ cm^{-2}. The irradiation is performed through a Mesh 400 TEM grid covering the sample (see Fig. 1,b), the bar periodicity is 63.5 µm with a bar width of 30 µm.

Therefore a bar pattern occurs on the sample. This bar pattern is used to investigate the sample by AFM and derive the swelling behavior. The influence of irradiation is studied consequently with a nanoindenter.

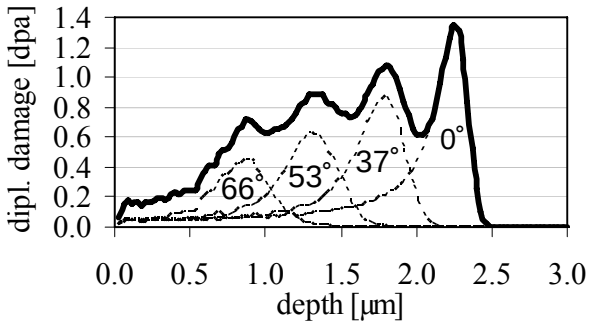

a

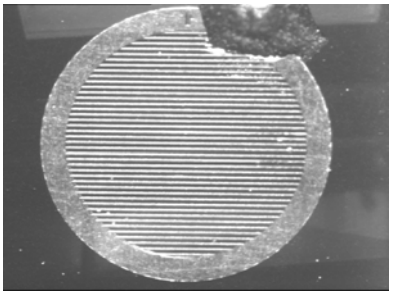

b

Fig. 1. a – TIRM simulation of the He implantation using 4 angles (0°, 37°, 53° and 66°) with a total He fluence of $5.6 \cdot 10^{16}$ cm^{-2} and an energy of 1.5 MeV. The single fluences for each angle (α) are: $\cos(\alpha) \cdot 2.0 \cdot 10^{16}$ cm^{-2}; b – ODS sample with Ni parallel bars (400 lines/inch)

2.3. AFM INVESTIGATIONS

The samples are investigated by atomic force microscopy, using an apparatus from Digital Instruments "Dimension 3100". The maximum scan region with the used AFM head is 124 x 124 µm with a maximum scanning depth of 6.6 µm. The depth resolution is mainly limited by noise. The scanning is performed in tapping mode, in order to reach higher precision and to avoid friction related artifacts of the irradiated surface. The sample preparation for the PM2000 is rather difficult, because the dispersed yttria nano-particles are pulled out during ceramographic preparation and scratch the surface. Therefore the AFM sometimes shows some artifacts on the scan. These peaks are removed with a computer program, and the resulting AFM images are well analyzable. In all cases the swelling is large enough to be well distinguishable from any noise and the remaining artifacts on the scan. An example of such an analysis is shown in Fig. 4,a. The x-direction of the scans is then averaged and a third order fit of two constantly separated curves is performed through the original and the swelled region (see Fig. 4,b).

2.4. NANO-INDENTATION

In order to test the mechanical behavior a nano-indenter from CSM Instruments SA in Neuchâtel (Switzerland) is applied, the maximum load of the apparatus being 500 mN with a load resolution of 0.04 µN and a maximum depth of 20 µm with a resolution of 0.04 nm. Two measurements series are performed using a Berkovich tip (a tetrahedron that comes to a sharp point). In both cases the indent depth is fixed. In the first series it is set to 500 nm, and in the second one to 1 µm. The targeted indent positions are localized with an optical microscope being connected to the indenter. The positioning is performed with a precision of about 1 µm. Two series of indents are performed on a sample irradiated with the dose and damage profile described in Fig. 1. In each series the indents are positioned such, that both, non irradiated and irradiated parts of the sample are tested. Figure 2 shows the first indentation series, where the two first indents are placed in the non-irradiated part, the following three in the irradiated part and the last one in a non-irradiated section on the other side of the irradiated stripe.

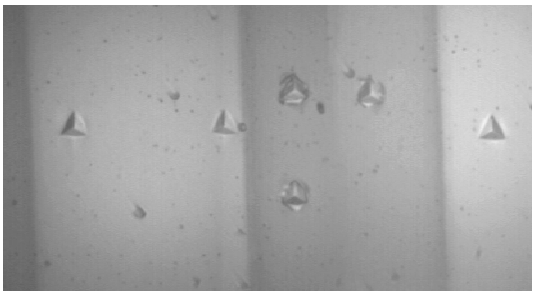

Fig. 2. First indent series with 500 nm penetration depth. The lighter surface displays the non irradiated part and the darker one the irradiated part of the sample

The reproducibility of the results is very good, as illustrated in Fig. 3. All load/penetration curves comply with each other in both, the irradiated and the non-irradiated area respectively.

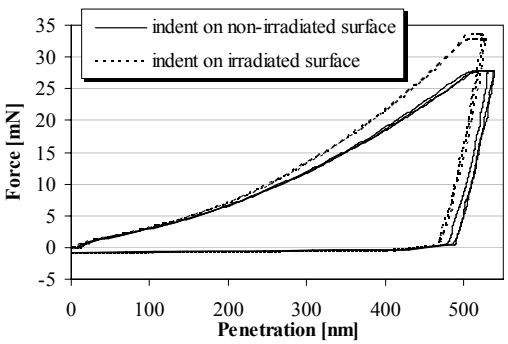

Fig. 3. Force to penetration depth characteristic of the 500 nm indents performed on the irradiated and the non-irradiated surfaces

3. RESULTS

3.1. SWELLING BEHAVIOR

The AFM shows the swelling pattern of the irradiated ODS bars. Figure 4,a shows a sample irradiated with He ions under the conditions described in Fig. 1,a. Figure 4,b is a third order fit through both, the irradiated and the non-irradiated parts of the profile. The swelling is deduced from the distance of the two fitted curves.

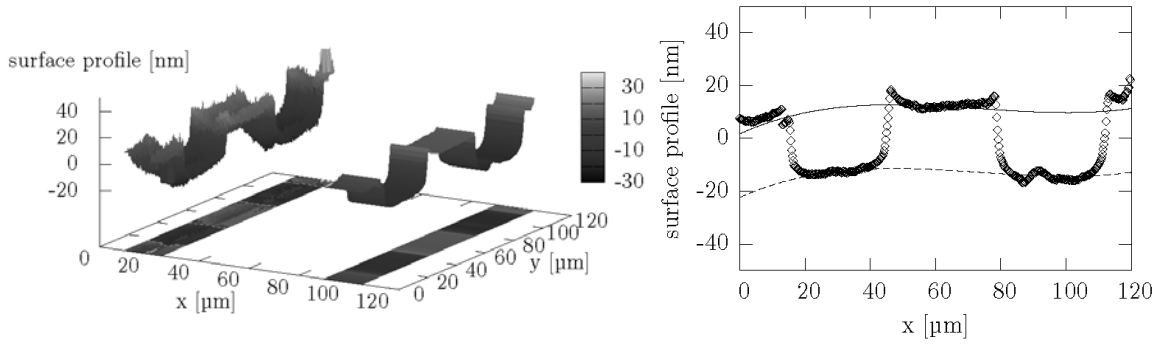

a *b*

Fig. 4. Surface of the ODS sample, investigated by AFM, original data after peak removal on the left side and the averaged profile on the right (a). Third order fitting through the averaged profile (b). Separate curves are derived for the irradiated and the non-irradiated locations on the profile, a step height of 24.1±2.8 nm is found for this example

Four different irradiation doses are applied (see 2.2). For each of the irradiated samples, the swelling is determined by AFM, resulting in a displacement dependency as a function of fluence. The displacements are shown in Fig. 5,a and they are represented as strain data in Fig. 5,b.

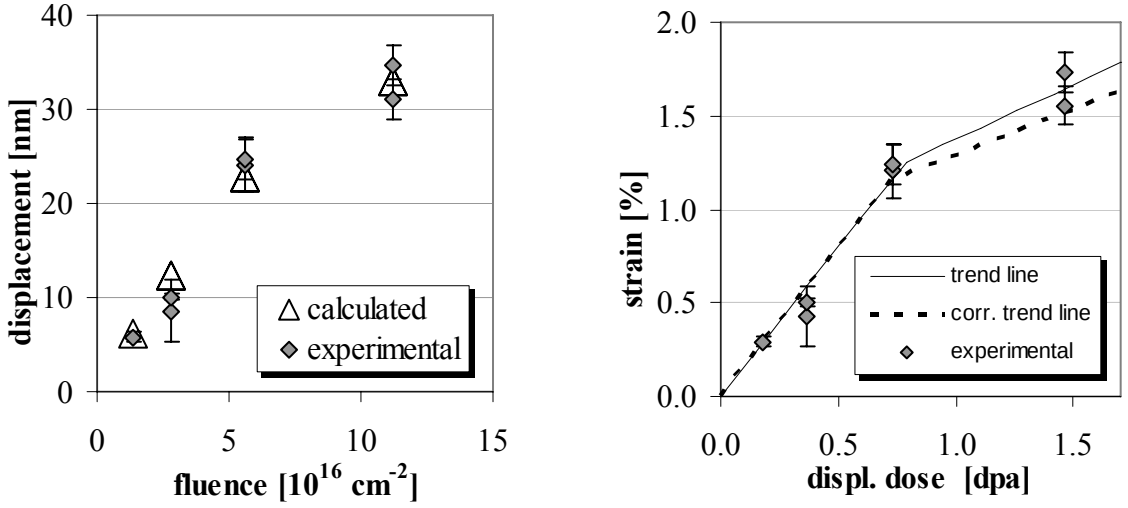

a *b*

Fig. 5. Swelling data as measured. The calculated data is based on the corrected strain trend line in (b) and the implanted profile with the strain profile in Fig. 6 (a). Strain data as function of the averaged displacements of the depth region from 0.5 to 2.5 µm with the corresponding trend line (b). The corrected trend line is based on the strain profile shown in Fig. 6 and shows the strain as a function of the exact (non-averaged) dpa value

The strain data are used to determine a bi-linear trend line. Because of the small amount of data points and for simplicity, this form of the trend line is chosen rather than a more sophisticated function. The x-axis for strain data and the trend line represents the average displacement in the depth from 0.5 to 2.5 µm. Because of the non-linearity of strain as a function of displacements and because of the displacement damage not being constant in the relevant depth region, the data points can not be assigned to the precise displacement value, but only to the average value for the actual displacement distribution. This distribution is depicted

in Fig. 6,a (solid thin line), the profile is directly obtained by overlying TRIM simulations for each incident angle.

TRIM tends to underestimate the profile width for the single simulations; therefore the initial profile is fitted with a polynomial of seventh degree. This polynomial is also presented in Fig. 6,a (doted line) and is used for further calculations. Fig. 6,a also shows the strain profile, which is calculated, using the corrected strain as a function of displacements shown in 5,b and the displacement polynomial. The corrected strain to displacement function is found on an iterative way, by introducing correction factors to the parameters of the trend line in Fig 5,b. By calculating the swelling of the known displacement distribution with the corrected strain to displacement function (integration), a direct comparison with the measured data can be performed (see Fig 5,a. Subsequently the parameters of the corrected trend line can be adjusted to reach a good matching of the experimental data points and the calculated ones.

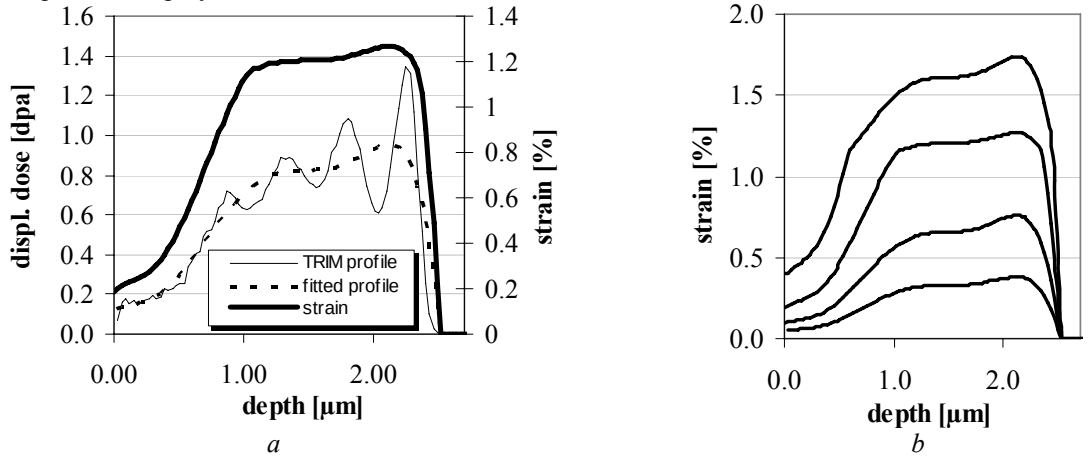

Fig. 6. Displacement profile for a fluence of $5.6 \cdot 10^{16}$ cm^{-2} calculated with TRIM and an averaged profile used for calculations (a). With the averaged profile and the corrected trend line of relative strain (see Fig. 5,b), the strain profile is calculated. All strain profiles for the different implantation fluence ($1.4 \cdot 10^{16}$, $2.8 \cdot 10^{16}$, $5.6 \cdot 10^{16}$ and $1.12 \cdot 10^{17} cm^{-2}$). Because of the non linearity of the strain to displacement function, the shape varies with the total fluence (b)

MECHANICAL PROPERTIES

In this paper the hardness is investigated using a nanoindenter, see Section 2.4. Results are presented for the non-irradiated and the irradiated surface of the sample. Figure 8 contains the results for both indentation series, the one with an indentation depth of 500 nm and the one with 1000 nm. For both series a consistent increase of the irradiation induced increase in hardness, can be observed. For the 1000 nm indent series, two indents are placed on the border line between the irradiated and the non-irradiated surface, accounting for mixed regions. Figure 7 shows such an indent, where about 40% of the indent is performed on an irradiated surface. The axis of abscissae in Fig. 8 does therefore not only contain the distinctive cases of non-irradiated and irradiated, but represents the percentage of the indent accounting for an irradiated region.

The intermediate data points properly fit between the distinctive cases. The hardness is compared to values reported in [8], in this thesis the hardness is measured by a Vickers indenter with a mass of 30 kg and a 2/3" objective. For untreated ODS samples a Vickers hardness of 326±6 HV30 is reported. Transforming this into Si units results in a hardness of 3197±59 MPa which agrees well with the result of 3207 MPa found for the 1000 nm indents on the non-irradiated surface (see Fig. 8).

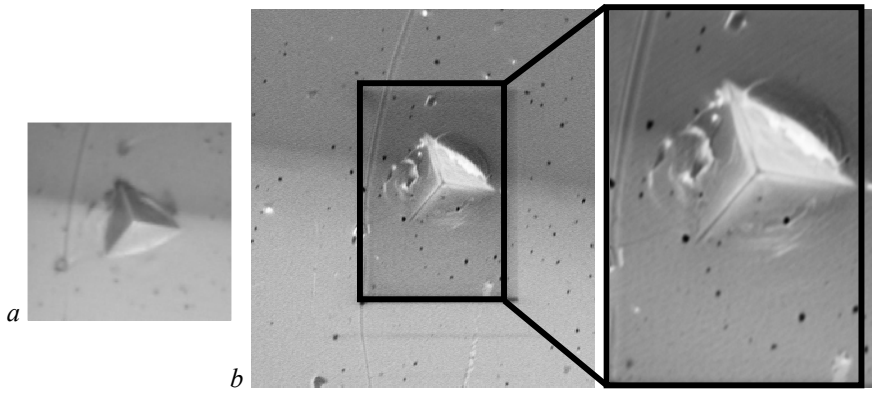

Fig 7. Optical (a) and SEM (b) picture of a 1 µm indent at the border between the irradiated and the non irradiated surface of the sample

In Fig. 8 the hardness decreases with increasing the indentation depth. The depth-dependent hardness has been observed in various materials such as metals, diamond-like carbon, polymers, ceramics, etc before. The depth-dependent hardness has been explained by the theory of strain-gradient plasticity and the surface effect [9].

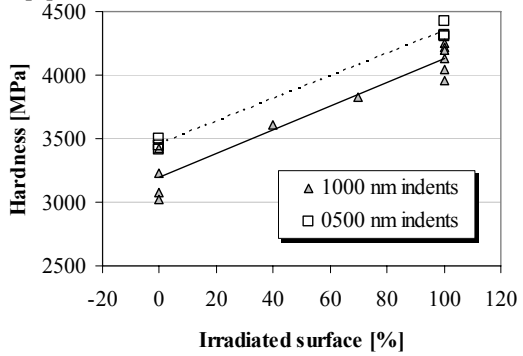

Fig. 8. Hardness as a function of the irradiated surface to non-irradiated surface fraction of the indentation region

4. DISCUSSION

The increased hardness of the irradiated surfaces well agrees with results for ferritic steels found in literature. In [10], low activation ferritic steel is investigated by micro-indentation technique in order to find the ion induced hardening. At an irradiation temperature of 673 K, irradiation-produced dislocation loops are observed by TEM, the number and density of these loops is clearly increased and their mean size is decreased with increasing He concentration. The irradiation induced micro hardness changes were no more than 10 at.%673 K. In this paper the irradiation induced hardness changes at room temperature are 29% for the 1000 nm indents and 26% for the 500 nm indents. This difference might be attributed to a superimposed effect of the compressive residual stresses in the samples being investigated in this work. However, the differences might only come from the different radiation conditions.

In the present study only the transverse grain direction is studied. As the material is anisotropic, the other grain orientations will also be investigated. In [8] the hardness was distinguished for the longitudinal and the perpendicular extrusion direction. Differences were mainly found for thermally treated samples, where the hardness generally decreased by up to 23% and the transversal extrusion direction was 10% harder than the longitudinal one. For the untreated samples the hardness was almost isotropic.

5. CONCLUSIONS

At room temperature and displacement dose ranges around 0.7 dpa, PM2000 already shows a major increase of its hardness by 30% and also a strain of around 1%. Annealing effects at higher temperatures will potentially decrease the hardening and swelling effects. Future experimental series will address this question. A first hint for a temperature decreased hardness can be found in [8,10], where the thermal treatment significantly decreased the hardness, and the irradiation induced hardening effect was reduced at higher temperatures.

The present work demonstrates that the nano/micro scale approach to characterize the material is valid. In case of the hardness a good agreement with literature data exists, and the swelling induced displacements are also within expectations.

6. ACKNOWLEDGEMENTS

The authors wish to thank Tomislav Rebac at the Paul Scherrer Instiute for his preparation of the ODS plates. The nano-indents were performed at the CMS Company in Neuchâtel by Philippe Kempe. The financial support of this project by the department Nuclear Energy and Safety of PSI is greatly acknowledged.

REFERENCES

1. S. Ukai and M. Fujiwara. Perspective of ODS alloys application in nuclear environments *//Journal of Nuclear Materials*. 2002, v. 307, p. 749–757.

2. D.T. Hoelzer, Contributors: G.R. Odette, M.J. Alinger, D.S. Gelles A.F. Rowcliffe, R.L Klueh, B.A. Pint, P.J. Mazias. Advanced Alloy Systems *//Fusion Materials Science peer review August 27-28.* 2001, University of California-Santa Barbara, http://www.fusionmaterials.pnl.gov/peerreview/hoelzer_advanced.pdf

3. Prof. L. Singheiser, private communication, January 2003.

4. M.A. Fütterer *//JRC Petten, private communication*, September, 2003.

5. A. Czyrska-Filemonowicz and B. Dubiel. Mechanically alloyed, ferritic oxide dispersion strengthened alloys: Structure and properties //*Journal of Materials Processing Technology.* 1997, v. 64(1-3), p. 53–64.

6. Dispersion-Strengthened High-Temperature Materials /*Material properties and applications, Prospectus from Plansee.* 2003, 706 DE.04.03(1000)RWF.

7. *ASTM Designation: E 521 – 96* /Standard Practice for Neutron Radiation Damage Simulation by Charged-Particle Irradiation.

8. V.A. Yardley. *Magnetic Detection of Microstructural Change in Power Plant Steels* /Dissertation at the University of Cambridge, May 2003, p. 261.

9. Xu, W.H. and T.Y. Zhang. *Surface effect for different types of materials in nanoindentation.* Advances in Fracture and Failure Prevention, Pts 1 and 2, 2004. 261-263, p. 1587–1592.

10. Y.Katoh et al. The influence of helium co-implantation on ion-induced hardening of low activation ferritic steel evaluated by micro-indentation technique //*Journal of Nuclear Materials*. 1999, v. 272, p. 115–119.

ОДУ СТАЛИ КАК КОНСТРУКЦИОННЫЕ МАТЕРИАЛЫ ДЛЯ ВЫСОКОТЕМПЕРАТУРНЫХ ЯДЕРНЫХ РЕАКТОРОВ

М.А. Пушон, М. Дюбели, Р. Шелдорф, Ж. Шен, В. Хёфельнер, С. Дегельдр

Окисно диспергированные упрочненные (ОДУ) ферритно-мартенситные стали изучались как возможные конструкционные материалы для нового поколения высокотемпературных ядерных реакторов с газовым охлаждением. Аустенитные ОДУ-суперсплавы на базе никеля не рассматривались из-за присутствия никеля, который нежелателен при нейтронном облучении. ОДУ-стали рассматривались как возможные заменители других высокотемпературных материалов для изготовления трубопроводов или других композиционных узлов. Интересно, что ОДУ рассматривается так же, как возможный кандидат для использования в термоядерных устройствах. Окисные частицы служат как межфазные ловушки для закрепления движущихся дислокаций. Поэтому сопротивление ползучести увеличивается. В случае использования этих материалов в реакторе их поведение под облучением должно изучаться более тщательно. В предлагаемой работе исследуются эффекты, обусловленные внедрением Не. Измеряется обусловленное распухание и механические характеристики облученной поверхности. Эти первые испытания были выполнены при комнатной температуре, когда можно явно наблюдать распухание и упрочнение.

ОДЗ СТАЛІ ЯК МОЖЛИВІ КОНСТРУКЦІЙНІ МАТЕРІАЛИ ДЛЯ ВИСОКОТЕМПЕРАТУРНИХ ЯДЕРНИХ РЕАКТОРІВ

М.А. Пушон, М. Дюбелі, Р. Шелдорф, Ж. Шен, Ф. Хофельнер, С. Дегельдр

Окисно дисперговані зміцнені (ОДЗ) феритно-мартенситні сталі досліджуються як можливі конструкційні матеріали для нового покоління високотемпературних ядерних реакторів з газовим охолодженням. Аустенітні ОДЗ-сплави на основі никелю не вивчаються завдяки никелю, присутність якого під дією опромінення небажана. ОДЗ-сталі разглядаються як можливі кандидати на заміну інших високотемпературних матеріалів для виготовлення трубопроводів або інших конструкційних вузлів. Цікаво, що ОДЗ-матеріали розглядаються також з точки зору їх можливого використання для майбутнього застосування в термоядерних пристроях. Окисні частки служать як міжфазні пастки для закріплення дислокацій, що рухаються. У разі використання ціх материалів в реакторі їх поведінка під опроміненням повинна вивчатись більш ретельно. В роботі досліджуються ефекти, зумовлені проникненням Не. Вимірюється зумовлене розпухання та механічні характеристики опроміненої поверхні. Ці перші дослідження були виконані при кімнатній температурі, коли можно чітко спостерігати розпухання та зміцнення.